Cosmological constraints on Hořava gravity revised in light of GW170817 and GRB170817A and the degeneracy with massive neutrinos

Noemi Frusciante[1] and Micol Benetti[2,3]

[1]*Instituto de Astrofísica e Ciências do Espaço, Faculdade de Ciências da Universidade de Lisboa, Edificio C8, Campo Grande, P-1749016, Lisboa, Portugal*
[2]*Dipartimento di Fisica "E. Pancini", Università di Napoli "Federico II," Via Cinthia, I-80126, Napoli, Italy*
[3]*Istituto Nazionale di Fisica Nucleare (INFN), sez. di Napoli, Via Cinthia 9, I-80126 Napoli, Italy*

(Received 8 February 2021; accepted 28 April 2021; published 26 May 2021)

We revise the cosmological bounds on Hořava gravity, taking into account the stringent constraint on the speed of propagation of gravitational waves from GW170817 and GRB170817A. In light of this, we also investigate the degeneracy between massive neutrinos and Hořava gravity. We show that a luminal propagation of gravitational waves suppresses the large-scale cosmic microwave background (CMB) radiation temperature anisotropies, and the presence of massive neutrinos increases this effect. On the contrary, large neutrinos mass can compensate the modifications induced by Hořava gravity in the lensing, matter, and primordial B-mode power spectra. Another degeneracy is found, at a theoretical level, between the tensor-to-scalar ratio r and massive neutrinos, as well as with the model's parameters. We analyze these effects using CMB, supernovae type Ia (SNIa), galaxy clustering, and weak gravitational lensing measurements, and we show how such degeneracies are removed. We find that the model's parameters are constrained to be very close to their general relativity limits, and we get a 2 orders of magnitude improved upper bound, with respect to the big bang nucleosynthesis constraint, on the deviation of the effective gravitational constant from the Newtonian one. The deviance information criterion suggests that in Hořava gravity, $\Sigma m_\nu > 0$ is favored when CMB data only are considered, while the joint analysis of all datasets prefers zero neutrinos mass.

DOI: 10.1103/PhysRevD.103.104060

I. INTRODUCTION

Theoretical [1–6] and observational [7–15] issues are challenging the cosmological standard model or Λ-cold-dark-matter (ΛCDM). Alternative proposals usually include an additional dynamical scalar degree of freedom (d.o.f.), thus entering in the realm of modified gravity (MG) theories [3,16–25]. The additional d.o.f. can be, among others, the result of breaking the Lorentz invariance (LI). Hořava gravity [26,27] is a Lorentz violating (LV) theory that breaks the LI by adding geometrical operators with higher order spatial derivatives to the action without including higher order time derivatives. The theory is then invariant under the more restricted foliation-preserving diffeomorphisms, $t \to \tilde{t}(t)$ and $x^i \to \tilde{x}^i(t, x^i)$, and it is power-counting renormalizable [28,29]. As such, it is a candidate for an ultraviolet completion of general relativity (GR). The general action is characterized by a potential $V(g_{ij}, N)$ that depends on the spatial metric g_{ij} and lapse function, N, of the Arnowitt-Deser-Misner (ADM) metric and their spatial derivatives. The power counting renormalizability allows the potential to contain only those operators, which are at least a sixth order in spatial derivatives in a four-dimensional space-time.

Different versions of Hořava gravity correspond to various forms of the potential (see Ref. [30] for a review). One can impose the lapse function to be only a function of time, $N = N(t)$, obtaining the so-called projectable version [27]. On the contrary, if the lapse is a function of both space and time, one has the nonprojectable version. Another option is that of detailed balance, which requires the potential to be derived from a superpotential [27]. Both the projectable and detailed balance versions limit the proliferation of operators allowed by the symmetry of the theory, but their assumption is not based on any fundamental principle, and, in some cases, they can lead to instabilities and strong coupling at low energies [30–39]. In the following, we will consider the low-energy cosmology of the nonprojectable version of the theory [40], which is free from these pathologies and shows a rich phenomenology compared to ΛCDM [41–49]. For instance, Hořava gravity induces a rescaling of the gravitational constant at the background level [45]. This impacts the relic abundance of elementary particles in the Universe [41] and enhances the growth of matter perturbations compared to ΛCDM [42,43]. LV also induces modification in the cosmic microwave background (CMB) power spectra through the

lensing, the integrated Sachs-Wolfe (ISW) effects, and a modified propagation of primordial gravitational waves (GWs) [42,47,48,50].

Hořava gravity is largely constrained by several probes, which span from local tests to astrophysical and cosmological ones. These include big bang nucleosynthesis (BBN) bounds [41,51]; vacuum Cherenkov bounds, which exclude subluminal propagation for both tensor and scalar polarizations to a very high accuracy [52]; post-Newtonian tests on the preferred-frame effects [48,53–57]; binary pulsars that can constrain the modification on the orbital dynamics due to the emission of dipolar radiation [58]; cosmological data [42,47,48] such as CMB, baryon acoustic oscillations (BAO), galaxy power spectrum, and supernovae Ia (SNIa) measurements; and by the time delay between the gamma-ray burst GRB170817A and the gravitational wave event GW170817 [59,60]. The latter sets a tight bound on the deviation of the speed of propagation of tensor modes, c_t^2, from the speed of light, c, of order 10^{-15}. It implies that one of the free parameters of Hořava gravity is found to be $\mathcal{O}(10^{-15})$, leading to a revision of the allowed parameter space [61].

In this work, we aim to revisit previous cosmological analysis on Hořava gravity by considering the GWs bound and providing updated bounds. Previous cosmological analyses take into account constraints from other sources (e.g., post-Newtonian tests, BBN, Cherenkov radiation) but not the tightest one from GWs. Thus, as a novelty, we assume the GWs constraint in its stringent form, *i.e.*, $c_t^2 = 1$ (in unit of $c = 1$). Moreover, we will extend previous works by including in the analysis massive neutrinos (with a varying mass) and investigating the degeneracy between Hořava gravity and massive neutrinos. It is well known that MG models can mimic the effects of massive neutrinos on observables and impact the constraints on their mass [62–70].

The paper is organized as follows. In Sec. II, we introduce the low-energy action of Hořava gravity and provide an overview of the current observational constraints on the model's parameters and stability relations. In Sec. III, we outline the methodology adopted and introduce the formalism and the numerical tools used. In Sec. IV, we discuss the degeneracy between massive neutrinos and Hořava gravity by looking at the scalar angular power spectra and matter power spectrum, as well as the primordial B-mode spectrum. In Sec. V, we present the cosmological constraints using the most updated datasets. Finally, we conclude in Sec. VI.

II. HOŘAVA GRAVITY

Let us consider the low-energy action of Hořava gravity [40] in the presence of matter fields, which can be written as follows:

$$\mathcal{S} = \frac{1}{16\pi G_H}\int d^4x\sqrt{-g}(K_{ij}K^{ij} - \lambda K^2 - 2\xi\bar{\Lambda} + \xi\mathcal{R} + \eta a_i a^i) + S_m[g_{\mu\nu},\chi_i], \tag{1}$$

where $g_{\mu\nu}$ is the metric tensor and g its determinant, $\mathcal{R}$ is the Ricci scalar of the three-dimensional spacelike hypersurfaces, K_{ij} is the extrinsic curvature, K is its trace, and $a_i = \partial_i \ln N$ is the three-vector defined in terms of the lapse function, N, of the ADM metric. The three free parameters $\{\lambda, \xi, \eta\}$ are dimensionless running coupling constants, and $\bar{\Lambda}$ is the so-called "bare" cosmological constant. We define S_m as the matter action for all matter fields, χ_i. We further define $G_H = \xi(1 - \frac{\eta}{2\xi})G_N$ [40] as the coupling constant, where G_N is the Newton gravitational constant. The GR limit is recovered when $\lambda = 1$, $\xi = 1$ and $\eta = 0$.

Action (1) propagates one scalar and two tensor modes, which have to satisfy some stability conditions. These require the avoidance of ghost instabilities and positive speeds of propagation for both scalar and tensor modes, which translate into the following requirements [40]:

$$0 < \eta < 2\xi, \qquad \lambda > 1. \tag{2}$$

Additional constraints on the model parameters can be found considering the bounds on the two parametrized post-Newtonian (PPN) parameters associated with the preferred frame effects, which are $|\alpha_1| \lesssim 3 \times 10^{-4}$ and $|\alpha_2| \lesssim 7 \times 10^{-7}$ at 99.7% C.L. [53,54]. These can be written in terms of the free parameters of the theory as follows [55–57]:

$$\alpha_1 = 4(2\xi - \eta - 2), \tag{3}$$

$$\alpha_2 = -\frac{(\eta - 2\xi + 2)(\eta(2\lambda - 1) + \lambda(3 - 4\xi) + 2\xi - 1)}{(\lambda - 1)(\eta - 2\xi)}. \tag{4}$$

From that, one can infer $\log_{10}(\lambda - 1) < -4.1$ at 99.7% C.L. [48]. Usually, the bounds in Eqs. (3)–(4) translate in

$$\eta = 2(\xi - 1), \tag{5}$$

and the parameter space reduces to a two-dimensional plane.

Assuming a flat Friedmann-Lemaître-Robertson-Walker (FLRW) background with line element

$$ds^2 = -dt^2 + a(t)^2\delta_{ij}dx^i dx^j, \tag{6}$$

where $a(t)$ is the scale factor and $\{t, x^i\}$ are, respectively, the time and spatial coordinates, the variation of the Action (1), with respect to the metric, provides the modified Friedmann equation, which reads

$$H^2 = \frac{G_c}{G_N} H_0^2 \left(\frac{\Omega_m^0}{a^3} + \frac{\Omega_r^0}{a^4} + \frac{8\pi G_N}{3H_0^2}\rho_\nu + \Omega_{\rm DE}^0 - 1 + \frac{G_N}{G_c} \right), \tag{7}$$

where $H \equiv \frac{1}{a}\frac{da}{dt}$ is the Hubble parameter, and H_0 is its present time value; $\Omega_i^0 \equiv 8\pi G_N \rho_i^0 / 3H_0^2$ are the dimensionless density parameters, and the subscript 0 stands for their present day values, where ρ_i stands for the density of baryons + cold dark matter (m), radiation (r), and massive neutrinos (ν); and the dark energy (DE) density parameter at present time, *i.e.*, $\Omega_{\rm DE}^0$, is defined from the flatness condition as follows [48]:

$$\Omega_{\rm DE}^0 = \frac{2\xi}{2\xi - \eta}\frac{\bar{\Lambda}}{3H_0^2} + 1 - \frac{3\lambda - 1}{2\xi - \eta}. \tag{8}$$

This definition allows us to express $\bar{\Lambda}$ in terms of $\Omega_{\rm DE}^0$ and to rewrite the Friedmann equation only in terms of the parameters that will be sampled. Additionally, the effective gravitational constant is [40,71]

$$G_c = \frac{(\eta - 2\xi)}{1 - 3\lambda} G_N. \tag{9}$$

The BBN constraint on the helium abundance [72–74] sets a bound on G_c, which is [41,51]

$$\left| \frac{G_c}{G_N} - 1 \right| < \frac{1}{8}, \tag{10}$$

and it can be used to further place bounds on the parameters of the theory. A combination of cosmological data, such as the CMB, local Hubble measurements, SNIa, galaxy power spectrum, and BAO measurements, sets an improved upper limit on the deviation of the cosmological gravitational constant from the local Newtonian one [48], which is $G_c/G_N - 1 < 0.028$ (at 99.7% C.L.) and even stronger when the PPN bounds are enforced, with $G_c/G_N - 1 < 6.1 \times 10^{-5}$ (99.7% C.L.).

The strongest constraint on the theory comes from the joint observations of the GW signal from a binary neutron star merger (GW170817) [59] and its gamma ray emission (GRB170817A) [60], which set a bound on the speed of propagation of tensor modes of $-3 \times 10^{-15} \leq c_t - 1 \leq 7 \times 10^{-16}$ [60]. In the case of Hořava gravity, it implies $|\xi - 1| \lesssim 10^{-15}$. The latter is several orders of magnitude stronger than the PPN bounds, and as such, it has been shown that the two-dimensional plane identified by the relation in Eq. (5) has to be substituted with the more informative two-dimensional plane $\{\eta, \lambda\}$, characterized by $\xi = 1$ [61]. In the present analysis, we will only impose *a priori* the GWs bound in the form $\xi = 1$, and we will not consider the condition in Eq. (5) in the following. In doing so, we aim to investigate the power in constraining of cosmological datasets when compared to other bounds, specially those from solar system.

Finally, let us note that the bare cosmological constant $\bar{\Lambda}$ can be substituted with the dark energy density parameter at present time in Eq. (8) [48]. Therefore, $\bar{\Lambda}$ will not be considered as a free parameter in the following analysis.

III. METHODOLOGY

The investigation of Hořava gravity at linear cosmological scales will be performed within the effective field theory (EFT) approach for dark energy and modified gravity [25,75–79], using the Einstein-Boltzmann code EFTCAMB [80–82]. The EFT formalism describes the evolution of MG theories with one additional scalar d.o.f. both at background and linear cosmological scales through a number of functions of time known as EFT functions. In this work, we will follow the methodology developed in Ref. [48], where the Hořava gravity model has been implemented in EFTCAMB, and we will use the resulting patch, which is publicly available.[1]

The EFT action for Hořava gravity with $c_t^2 = 1$, up to second order in perturbations, reads

$$\begin{aligned} \mathcal{S}_{\rm EFT} = \int d^4x\sqrt{-g}\Big\{ & \frac{m_0^2}{2}(1+\Omega)R + \Lambda(t) - c(t)\delta g^{00} \\ & - \frac{c(t)}{4}(\delta g^{00})^2 - \frac{\bar{M}_2^2}{2}(\delta K)^2 \\ & + m_2^2 h^{\mu\nu}\partial_\mu(g^{00})\partial_\nu(g^{00}) \Big\} + S_m[g_{\mu\nu}, \chi_i], \end{aligned} \tag{11}$$

where m_0^2 is the Planck mass, R is the 4D Ricci scalar, $\delta g^{00}, \delta K$ are the perturbations, respectively, of the upper time-time component of the metric and the trace of the extrinsic curvature, and $h^{\mu\nu} = (g^{\mu\nu} + n^\mu n^\nu)$ is the induced metric, with n_μ being the unit vector perpendicular to the time slicing. $\Omega, c, \Lambda, \bar{M}_2^2, m_2^2$ are the EFT functions. We note that Λ and c can be expressed in terms of Ω, H, and the densities and pressures of matter fluids by using the background field equations (see Refs. [75,76] for details) and the remaining three EFT functions are [48,83]

$$1 + \Omega = \frac{2}{(2-\eta)}, \tag{12}$$

$$\bar{M}_2^2 = -2\frac{m_0^2}{(2-\eta)}(1-\lambda), \tag{13}$$

$$m_2^2 = \frac{m_0^2 \eta}{4(2-\eta)}. \tag{14}$$

We refer the reader to Ref. [48] for further details about the background and linear perturbation equations implemented in EFTCAMB.

[1]Web page: http://www.eftcamb.org.

TABLE I. Table with the values of λ and η parameters for Hořava gravity that we consider in Sec. IV. We note that in this work, $\xi = 1$. Correspondingly, we include also the cases with massive neutrinos. The cosmological parameters are $\Omega_b^0 h^2 = 0.0226$, $\Omega_c^0 h^2 = 0.112$, with $h = H_0/100$, and $H_0 = 70$ km/s/Mpc. These cases study have been chosen to quantify the modification, with respect to ΛCDM, and the degeneracy with massive neutrinos.

Model	$\lambda - 1$	η	Σm_ν (eV)
H1	0.004	0.01	–
H1 + ν	0.004	0.01	0.85
H2	0.04	0.01	–
H2 + ν	0.04	0.01	0.85
H3	0.004	0.1	–
H3 + ν	0.004	0.1	0.85

The first part of our analysis will be the study of the impact of massive neutrinos on the cosmological observables and any degeneracy that might arise between massive neutrinos and the modifications of gravity induced by LV. In detail, we list in Table I the values of the parameters for Hořava gravity for the cases $H1$, $H2$, and $H3$ without massive neutrinos and $H1 + \nu$, $H2 + \nu$ and $H3 + \nu$ with the summed neutrino mass $\sum m_\nu = 0.85$ eV. These values are bigger than the observational constraints we will present in Sec. V and PPN bounds, and they serve only to visualize and quantify the modifications. As a reference, in our analysis, we always include the ΛCDM model.

Finally, we will perform a Markov Chain Monte Carlo (MCMC) analysis using the EFTCosmoMC code [81] and the datasets employed are listed in Sec. V A.

IV. DEGENERACY BETWEEN MASSIVE NEUTRINOS AND HOŘAVA GRAVITY: A PHENOMENOLOGICAL DESCRIPTION

Massive neutrinos have extended and measurable effects on the distribution of the large-scale structures, the CMB, and the expansion history [84–86]. Their impact depends strictly on the value of their mass. The latest measured value of the summed neutrino mass from the CMB Planck 2018 release sets the upper bound at $\Sigma m_\nu < 0.12$ eV (95% C.L. with Planck TT, TE, EE + lowE + lensing + BAO) in the context of a flat standard cosmological model [15], while the latest direct measurement from KATRIN experiment sets a higher upper limit of 1.1 eV at 90% C.L. [87].

In detail, massive neutrinos can change the height of the first acoustic peak of the CMB temperature-temperature power spectrum due to the early integrated Sachs Wolfe (ISW) effect, suppress the weak lensing effect, and dump the growth of structure on small scales [88]. Similar effects are also characteristic of DE and MG models, and, as such, a degeneracy between massive neutrinos and those models exists that strictly depends on the DE and MG models considered [62–70].

In the following, we show the imprint massive neutrinos leave on the dynamics of linear scalar and tensor perturbations in the context of Hořava gravity, and we investigate the degeneracy between massive neutrinos and the modified cosmological model under consideration. To this purpose, we also include the case without massive neutrinos and, for comparison, the ΛCDM model. For a complete overview of the cosmological effects of Lorentz violations, we refer the reader to [41–44,46,48,49,89] and to [45,47] for details about the effects of dark matter coupling with the aether.

A. Scalar angular power spectra and matter power spectrum

We discuss the impact of the nonzero massive neutrino component on the scalar angular power spectra of CMB anisotropy and the matter power spectrum. The results are in Fig. 1, where, in the top left panel, we show the low-ℓ tail of the CMB temperature-temperature power spectrum. We note that Hořava gravity models with a luminal propagation of GWs predict a suppressed ISW tail for $\ell < 30$, with respect to ΛCDM, which can be up to 16%. The $H1$ model is the closer one to ΛCDM, then, the $H2$ characterized by a larger value of λ (and same η), and finally, the $H3$, which has the largest value of η and the same value of λ as in $H1$. This feature is due to the late time ISW effect, *i.e.*, a modification of the time derivative of the lensing potential, $\dot{\Psi} + \dot{\Phi}$ (where Φ and Ψ are the gravitational potentials). In the specific case of Hořava gravity, $\dot{\Psi} + \dot{\Phi}$ results to be enhanced at a late time, with respect to ΛCDM. We note that the MG effect goes in the same direction of those of massive neutrinos. The latter indeed emphasizes the suppression. In $H1 + \nu$, massive neutrinos reduce the ISW tail of an additional ∼3.8%, with respect to the same model without massive neutrinos; in $H2 + \nu$, it is ∼6%, and in $H3 + \nu$, it is ∼5.5%. In ΛCDM + ν, massive neutrinos also lower the low-ℓ tail, with respect to the case without massive neutrinos of a factor up to 3.2%. Thus, in the case of Hořava gravity, the combined effects of massive neutrinos and modifications of gravity enhance the suppression. For $30 < \ell < 50$, the TT power spectra of $H1, H2$ ($+\nu$) strictly follow ΛCDM or are slightly suppressed, while the one of $H3$ model is enhanced. At these angular scales, the enhancement of $H3$ is lowered when massive neutrinos are included, compensating the MG effects.

At high ℓ in the TT power spectrum, the MG effects are different than those of massive neutrinos. The former act on the height of the CMB peaks; e.g., we note a lower amplitude of the first and second peaks compared to ΛCDM for larger values of λ ($H2$) or larger value of η ($H3$) due to a suppression of $\dot{\Psi} + \dot{\Phi}$ at early times. This suppression is more pronounced for the $H2$ case as modifications in the early ISW can be spotted already at $a \sim 10^{-3}$. The shift to higher multipoles in the position of the first two peaks is due to a different background

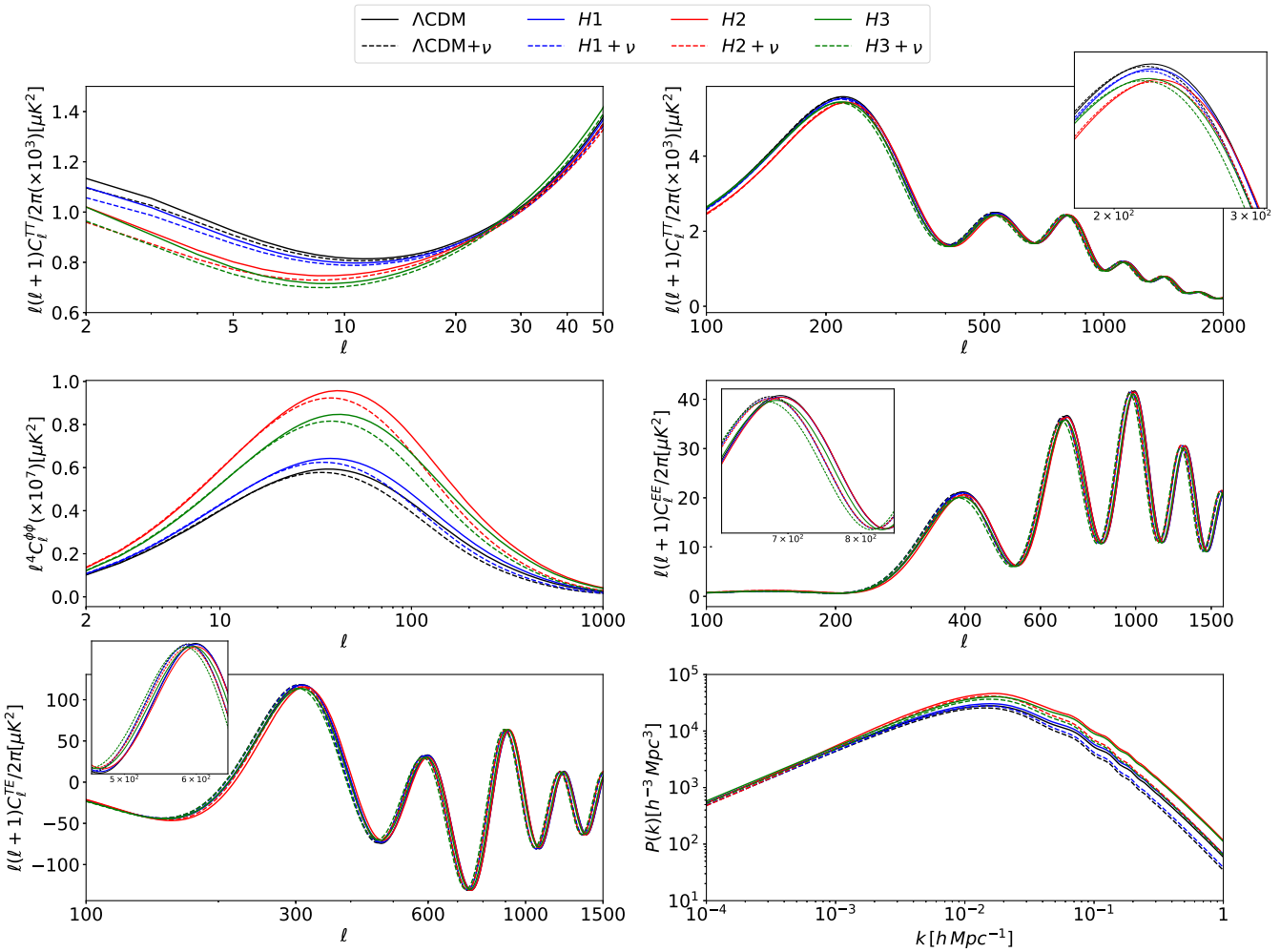

FIG. 1. Power spectra of different cosmological observables for the Hořava gravity models in Table I and ΛCDM. Top panels: CMB temperature-temperature power spectrum at low ℓ (left) and high ℓ (right). Central panels: Lensing potential autocorrelation power spectrum (left) and E-modes power spectra (right). Bottom panels: Cross-power spectra of the temperature anisotropies and E-mode polarization (left) and matter power spectra (right).

expansion, which is more pronounced in the $H2$ model, having $G_c = 0.94G_N$. On the contrary, massive neutrinos impact the position of the peaks by shifting the spectrum to lower multipoles for $\ell > 200$, due to a change in the background expansion history. Thus, a nonzero neutrinos mass can compensate the shift to higher ℓ in the CMB temperature anisotropy spectrum introduced by large value of the Hořava gravity parameters.

Hořava gravity models have an enhanced amplitude in the lensing power spectrum, with respect to ΛCDM at all multipoles, as shown in the left central panel in Fig. 1. The deviation is larger for $H2$ (∼90%), then it follows $H3$ (∼75%), and finally, $H1$ (12%). Massive neutrinos, as expected, lower the amplitude for $\ell > 20$ and, as in the case of the TT power spectrum, the effect is larger for $H2 + \nu$ and $H3 + \nu$ compared to both $H1 + \nu$ and $\Lambda\text{CDM} + \nu$.

In the right central panel in Fig. 1, we show the EE-power spectrum. $H1$ model does not show any sizable effect due to MG, with respect to ΛCDM. A larger value of λ ($H2$) introduces an enhancement for $\ell < 200$, which is $\lesssim$20%, with respect to ΛCDM, and then a suppression of the same order up to $\ell < 500$. A larger value of η, as it is the case of $H3$, instead modifies the shape of the peaks and troughs for $\ell > 400$ of about 10%. Massive neutrinos shift the overall spectrum to lower multipoles. In the TE-power spectra, the effects of MG are present for $\ell < 500$; see left bottom panel in Fig. 1. These include both a shift of the position of the peaks to high ℓ, with respect to ΛCDM and in the height of peaks and troughs. The difference is larger for $H2$ and $H3$, reflecting the effects in both the TT and EE power spectra. For the same reason, massive neutrinos shift the spectrum to lower multipoles. The recent Planck data 2018 show an improved treatment on foregrounds and systematic effects on both TT and polarization spectra at high multipole, and also on EE spectra at low ℓ, which can help in constraining these effects [90,91].

Finally, in the right bottom panel in Fig. 1, we show the matter power spectrum. The latter is enhanced for all Hořava gravity models, with respect to ΛCDM. The larger deviation is for $H2$, while massive neutrinos suppress the growth of structures as expected [88]. Thus, the resulting effect is to mitigate the modifications due to large values of the Hořava parameters.

Let us stress that the large deviations, with respect to ΛCDM, are a consequence of the big values of the parameters we have selected for $H1$, $H2$, and $H3$. While these are larger than actual bounds, these are very useful to amplify the effect on the spectra and visualize the degeneracy. Thus, the entity of the modifications that have been described in this section are specific to the choice of parameters, but the overall directions of the modifications with respect to ΛCDM and impact of massive neutrinos, hold for viable values of the parameters within the PPN and cosmological bounds.

B. Primordial B-mode spectrum

In this section, we discuss the Hořava gravity phenomenology and that of massive neutrinos on the primordial B spectrum of the CMB.

The Hořava gravity evolution for tensor modes h^T_{ij}, with $\xi = 1$ in Fourier space, is given by the following equation:

$$\ddot{h}^T_{ij} + 3H\dot{h}^T_{ij} + \frac{k^2}{a^2}h^T_{ij} + \frac{2-\eta}{2m_0^2}\delta T^T_{ij} = 0, \qquad (15)$$

where dots are derivatives, with respect to cosmic time, and δT_{ij} is the linear perturbation of the tensor component of anisotropic stress, which contains the neutrinos and photons contribution. The above equation is directly modified, with respect to the one for ΛCDM, because of the $2-\eta$ coefficient, which regulates the coupling between tensor modes and matter perturbations. Let us also note that although the friction term, $3H$, is not directly modified, the evolution of the Hubble parameter in the Hořava gravity model is rescaled by G_c, with respect to ΛCDM, thus affecting the amplitude of tensor modes. The combination of these effects leads to the features shown in Fig. 2. While the BB-power spectrum for $H1$ mostly overlaps with the ΛCDM one, both the $H2$ and $H3$ models show a general suppression of the peaks and troughs and a shift toward small ℓ. The overall differences are within 5% and are larger for the $H2$ model because it has the smaller values of G_c (for $H1$, $G_c = 0.99G_N$, for $H2$, $G_c = 0.94G_N$, and for $H3$, $G_c = 0.95G_N$). The inclusion of massive neutrinos further suppresses the first peak, and for larger multipoles ($\ell < 300$), the BB spectra are enhanced, a peculiar characteristic of massive neutrinos. They shift further the spectra toward smaller multipoles.

The total spectra including lensing are shown in Fig. 3. As already discussed in the previous section, the lensing potential is modified, resulting in an enhancement of the

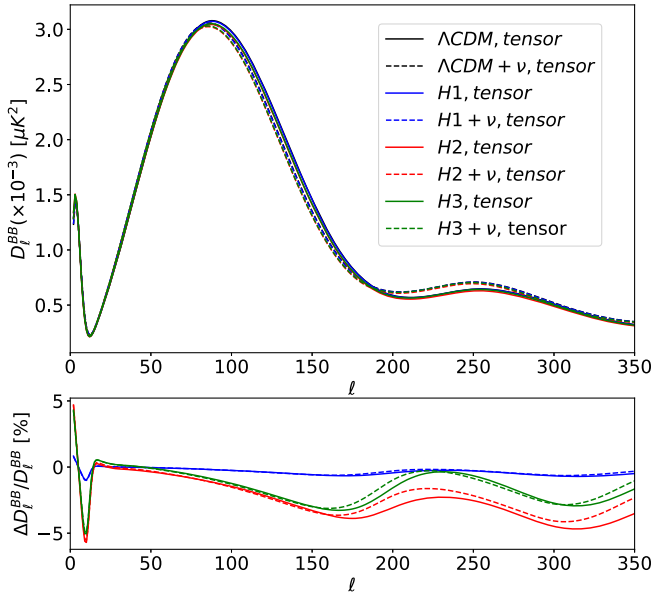

FIG. 2. The tensor contribution to the primordial BB power spectra for the Hořava gravity models in Table I and ΛCDM. We have set $r_{0.002} = 0.05$. We define $D_\ell^{BB} = \ell(\ell+1)C_\ell^{BB}/2\pi$ and the relative difference as $\Delta D_\ell^{BB}/D_\ell^{BB}$, *i.e.*, the difference between the Hořava gravity model and ΛCDM, divided by the standard cosmological model.

BB spectra for the Hořava gravity models, with respect to ΛCDM. The inclusion of massive neutrinos suppresses the tensor modes at high ℓ, reducing the effects of MG. We can infer that deviations due to large values of the Hořava gravity parameters can be compensated by the inclusion of massive neutrinos. Thus, in the BB-power spectrum, a degeneracy between massive neutrinos and the parameters of Hořava gravity also exists. Furthermore, we notice that the modified total BB-spectra can accommodate the

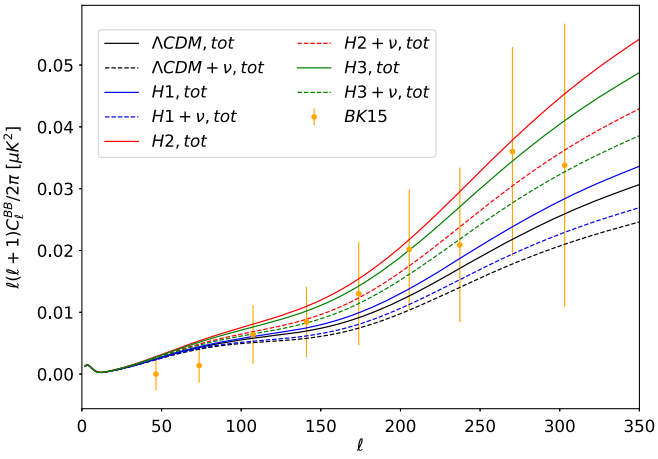

FIG. 3. The primordial total BB spectra, including lensing for the Hořava gravity models in Table I and ΛCDM. We also include the data points from BICEP2 and Keck Array (BK15) [92]. We have set $r_{0.002} = 0.05$.

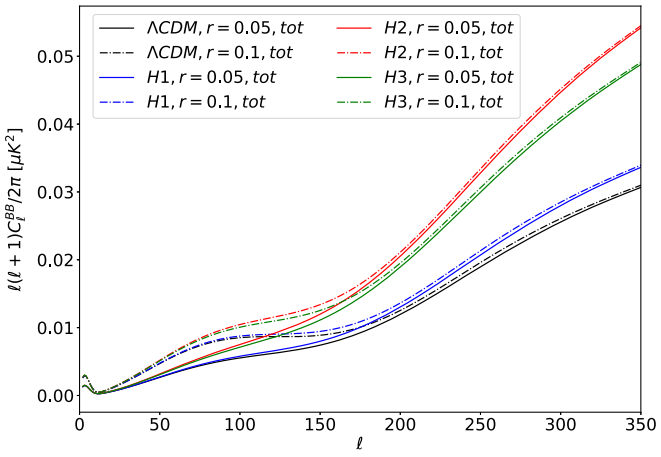

FIG. 4. The primordial total BB spectra, including lensing for the Hořava gravity models is Table I and ΛCDM. We show the impact of different values of the ratio of the tensor-to-scalar power spectra, r, on the total BB spectra. We have chosen at the pivot scale, $k_* = 0.002$ h/Mpc, two values for $r_{0.002}$: $r_{0.002} = 0.05$ and $r_{0.002} = 0.1$.

BICEP2/Keck data points at high multipoles better than ΛCDM. In particular, the case of ΛCDM seems to worsen the fit to data at small angular scales, even though it stays within the error. We will show in Sec. V B that, indeed, this is the case. The joint analysis with CMB data shows a slightly better fit to data for Hořava gravity with a nonzero neutrinos mass.

Finally, we investigate the degeneracy between the tensor-to-scalar ratio r and the Hořava gravity parameters. r has indeed been proven to be degenerate with modifications of gravity, as it is the case of modifications due to a nonstandard friction term [93]. In Fig. 4, we show the impact of this parameter on the total BB-power spectrum. Regardless of the cosmological model, changing the value of r at the pivot scale $k_* = 0.002$ h/Mpc from $r_{0.002} = 0.05$ to $r_{0.002} = 0.1$ leads to an overall enhancement of the total BB-power spectra at all angular scales. However, the largest impact is for $\ell < 150$. Such enhancement is not only degenerate with the parameters of Hořava gravity as they can also lead to a larger amplitude of the BB-power spectrum at these angular scales, but also with massive neutrinos. The latter, indeed, can compensate a larger value of r as their effect is to dampt the BB-power spectrum amplitude. BICEP2/Keck data at low ℓ can, in principle, disentangle the degeneracy with r.

V. COSMOLOGICAL CONSTRAINTS

A. Datasets

In the present analysis, we consider the following datasets:

(i) Measurements of the B-modes CMB power spectrum from the BICEP2 and Keck Array experiments, including the 2015 observing season [92] (hereafter, "BK15");

(ii) CMB measurements, through the Planck (2018) data [91], using "TT, TE, EE + lowE" data by combination of temperature power spectra and cross-correlation TE and EE over the range $\ell \in [30, 2508]$, the low-ℓ temperature Commander likelihood, and the low-ℓ SimAll EE likelihood. We refer to this data set as "Plk18";

(iii) The lensing reconstruction power spectrum from the latest Planck satellite data release (2018) [91,94], hereafter, indicated with "lens";

(iv) Supernovae Type Ia data from the Joint Light-curve "JLA" sample [95], constructed from supernova legacy survey (SNLS) and Sloan digital sky survey (SDSS), and consisting of 740 data points covering the redshift range $0.01 < z < 1.3$. It is worth mentioning that JLA sample, compared to other recent SNIa compilations, has the advantage of allowing the light-curve recalibration with the model under consideration, which is an important issue when testing alternative cosmologies [96,97].

(v) Pantheon compilation [98] of 1048 SNIa in the redshift range $0.01 < z < 2.3$. This is a larger sample than JLA that combines the subset of 276 newPan-STARRS1 SNIa with useful distance estimates of SNIa from SNLS, SDSS, low z, and Hubble space telescope (HST) samples. It provides accurate relative luminosity distances. Hereafter, we indicate this dataset with "Pth";

(vi) Dark energy survey year one (DES-1Y) results that combine galaxy clustering and weak gravitational lensing measurements, using 1321 square degrees of imaging data [99]. We refer to this dataset as "DES."

For the analysis, we consider the following combinations: BK15 + Plk18, hereafter, BKP, which will be the baseline dataset; on top of it, we include first lens, DES and Pantheon (BKP + lens + DES + Pth), and then we consider JLA in place of Pantheon (BKP + lens + DES + JLA).

For the MCMC likelihood analysis, we use the EFTCosmoMC code [81]. We consider the Hořava gravity base model with a fixed $\xi = 1$ to satisfy GWs constraints and varying λ and η. For the latter, we consider flat priors: $\log_{10}(\lambda - 1) \in [-13, 0.1]$ and $\log_{10}\eta \in [-13, 0.1]$. The adopted ranges are consistent with stability conditions, which, in any case, are automatically enforced by the stability module of EFTCAMB [83,100,101]. We use a logarithmic sampler for these parameters following Ref. [48]. In addition to the model's parameters, we vary the physical densities of cold dark matter $\Omega_c h^2$ and baryons $\Omega_b h^2$, the angular size of the sound horizon at recombination $\theta_{\rm MC}$, the reionization optical depth τ, the primordial amplitude $\ln(10^{10} A_s)$ and spectral index n_s of scalar perturbations, and the tensor-to-scalar ratio r. We also consider the additional case of a varying summed neutrino mass Σm_ν.

TABLE II. Marginalized constraints on cosmological parameters at 68% C.L.; the upper limits are at 95% C.L.

Model	σ_8^0	Ω_m^0	H_0	$r_{0.002}$	Σm_ν (eV)
ΛCDM (BKP)	0.826 ± 0.008	0.310 ± 0.008	67.80 ± 0.61	<0.054	–
ΛCDM (BKP + lens + DES + Pth)	0.819 ± 0.006	0.297 ± 0.006	68.80 ± 0.47	<0.061	–
ΛCDM (BKP + lens + DES + JLA)	0.819 ± 0.006	0.297 ± 0.006	68.81 ± 0.47	<0.064	–
ΛCDM + ν (BKP)	0.811 ± 0.016	0.319 ± 0.012	67.11 ± 0.91	<0.058	<0.211
ΛCDM + ν (BKP + lens + DES + Pth)	0.809 ± 0.010	0.303 ± 0.008	68.31 ± 0.61	<0.065	<0.139
ΛCDM + ν (BKP + lens + DES + JLA)	0.809 ± 0.010	0.303 ± 0.008	68.28 ± 0.68	<0.065	<0.149
Hořava (BKP)	0.826 ± 0.008	0.313 ± 0.009	67.59 ± 0.64	<0.055	–
Hořava (BKP + lens + DES + Pth)	0.819 ± 0.006	0.298 ± 0.006	68.74 ± 0.47	<0.063	–
Hořava (BKP + lens + DES + JLA)	0.820 ± 0.006	0.298 ± 0.006	68.71 ± 0.47	<0.063	–
Hořava + ν (BKP)	0.818 ± 0.011	0.319 ± 0.009	67.09 ± 0.66	<0.055	<0.125
Hořava + ν (BKP + lens + DES + Pth)	0.810 ± 0.009	0.303 ± 0.007	68.26 ± 0.57	<0.060	<0.130
Hořava + ν (BKP + lens + DES + JLA)	0.810 ± 0.011	0.303 ± 0.008	68.25 ± 0.66	<0.060	<0.165

B. Results

This section is dedicated to the discussion of the cosmological and model parameters constraints of Hořava gravity. We consider both the model with and without massive neutrinos. For reference, we also include the results for ΛCDM in these two scenarios. We present the results of a selection of the cosmological parameters today $\{\Omega_m^0, H_0, \sigma_8^0, r_{0.002}, \Sigma m_\nu\}$ in Table II at 68% C.L. In Table III, we include the constraints on the model parameters, the derived constraints on α_1, α_2, and the deviation of the effective gravitational constant, G_c, from G_N at 68% C.L.

In Fig. 5, we show the marginalized likelihood of the cosmological parameters for ΛCDM (top panel) and Hořava gravity (bottom panel). The cosmological parameters of Hořava gravity are consistent with those of the ΛCDM model (see Table II). In both models, the BKP dataset prefers a slightly larger central value for Ω_m^0, with respect to the other two combinations (BKP + lens + DES + Pth, BKP + lens + DES + JLA). Because of the anticorrelation between Ω_m^0 and H_0, larger values of Ω_m^0 select smaller values of H_0 and vice versa. We show this feature in Fig. 6, where we see that the same holds in the case massive neutrinos are included. In the case of Hořava + ν, we note that the Ω_m^0 upper limit (at 95% C.L.) is slightly smaller, with respect to ΛCDM + ν for the BKP dataset, which, in turn, selects a higher lower limit for H_0. The anticorrelation also explains why H_0 goes toward smaller values when massive neutrinos are included. In this case, indeed, a larger value of Ω_m^0 is expected. We also note that the extended datasets prefer lower central values of Ω_m^0 (and higher values of H_0) in

TABLE III. The 68% C.L. marginalized posterior bounds on the Hořava and PPN parameters and the deviation of the effective gravitational constant from G_N. Upper limits indicated are at 95% C.L.. We have also included the results for the ΔDIC.

Hořava			
Parameters	BKP	BKP + lens + DES + Pth	BKP + lens + DES + JLA
$\log_{10}(\lambda - 1)$	-5.7 ± 2.9	< -3.2	< -3.1
$\log_{10}\eta$	< -2.8	< -2.7	< -2.9
α_1	> -0.008	> -0.008	> -0.010
α_2	<67	$<1.00 \times 10^6$	$<2.85 \times 10^6$
$(G_c/G_N - 1)$	$<0.35 \times 10^{-2}$	$<0.19 \times 10^{-2}$	$<0.27 \times 10^{-2}$
ΔDIC	6.1 (Moderate evidence)	3.7 (No evidence)	3.9 (No evidence)
Hořava + ν			
Parameters	BKP	BKP + lens + DES + Pth	BKP + lens + DES + JLA
$\log_{10}(\lambda - 1)$	$-2.6^{+0.1}_{-6.7}$	< -2.8	< -2.8
$\log_{10}\eta$	$-6.9^{+3.6}_{-3.0}$	$-6.0^{+3.4}_{-1.6}$	$-7.0^{+3.7}_{-3.0}$
α_1	> -0.006	> -0.008	> -0.007
α_2	$<0.18 \times 10^3$	$<0.48 \times 10^4$	$<0.28 \times 10^6$
$(G_c/G_N - 1)$	$<0.44 \times 10^{-2}$	$<0.22 \times 10^{-2}$	$<0.28 \times 10^{-2}$
ΔDIC	−0.4 (No evidence)	0.7 (No evidence)	4.1 (No evidence)
$\mathrm{DIC}_{\mathrm{Hor}+\nu} - \mathrm{DIC}_{\mathrm{Hor}}$	−3.0 (No evidence)	0.5 (No evidence)	3.1 (No evidence)

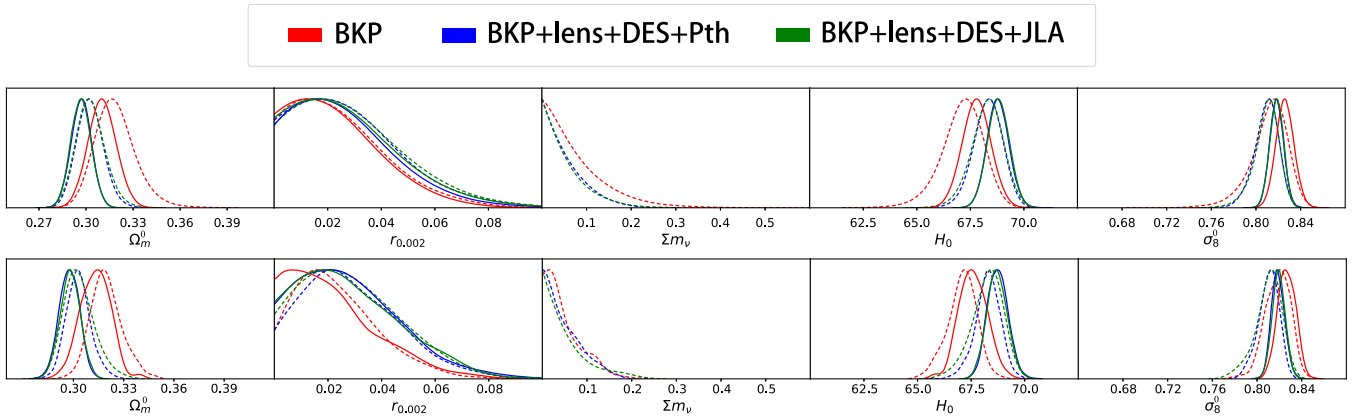

FIG. 5. Comparison between the ΛCDM (top panel) and Hořava gravity (bottom panel) marginalized cosmological parameters. Solid lines indicate the massless neutrino assumption, while dashed lines indicate the massive neutrinos extensions. The 68% C.L. are reported in Table II.

both cosmologies. We note that in the case of Hořava + ν, the dataset with JLA shows a higher upper bound for Ω_m^0 (< 0.323 at 95% and smaller lower limit for $H_0 > 66.68$ at 95%), with respect to the dataset with Pth ($\Omega_m^0 < 0.318$ and $H_0 > 67.05$). The distinction between JLA and Pth is not present in ΛCDM. This is due to the fact that the Hořava posterior of massive neutrinos (see central bottom line in Fig. 5 and Table II) for the dataset with JLA shows a higher upper limit with respect to ΛCDM. A similar consideration holds also for the baseline dataset, but, in this case, the upper limit is smaller than the ΛCDM case as it is the upper bounds for massive neutrinos in the Hořava gravity case.

Furthermore, in Fig. 7, we show the marginalized 2D joint distribution for H_0 and σ_8^0. We note that the inclusion of massive neutrinos introduces a correlation between these two parameters, which is more pronounced in the standard cosmological model. We note that being that the values of the cosmological parameters in Hořava gravity are compatible with those of ΛCDM within the errors, Hořava gravity suffers of the H_0 [7,9,99,102] and σ_8^0 [103] tensions, which characterize the standard ΛCDM scenario.

The bounds on the tensor-to-scalar ratio are the same in Hořava gravity and ΛCDM independently on the presence

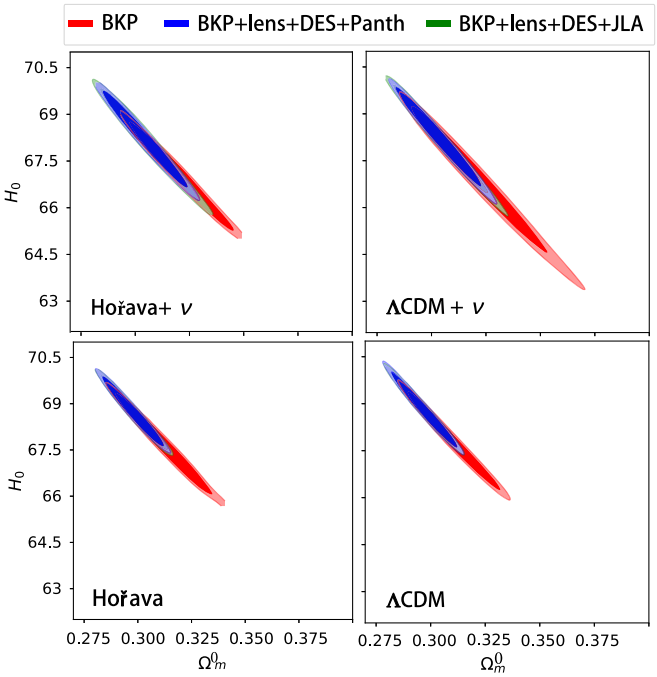

FIG. 6. $H_0 - \Omega_m^0$ plane for ΛCDM analysis (right panels) and Horava gravity model (left panels).

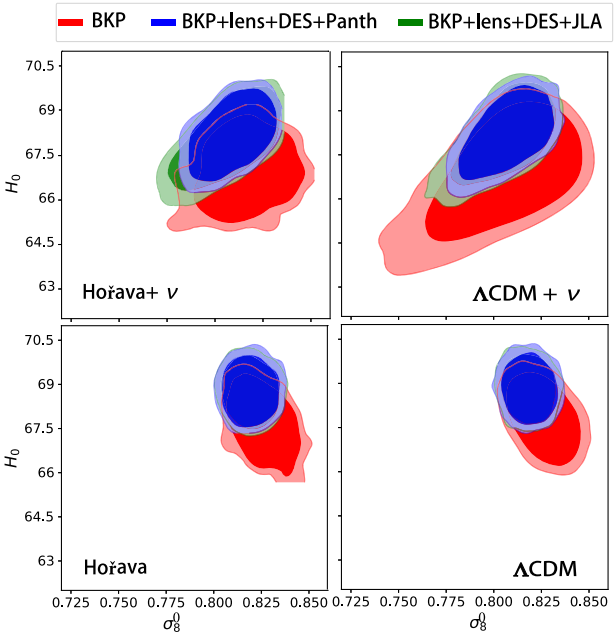

FIG. 7. $H_0 - \sigma_8^0$ plane for ΛCDM analysis (right panel) and Horava gravity model (left panel).

of massive neutrinos. The data analysis shows that the degeneracy between r, Σm_ν, and the Hořava gravity parameters discussed in Sec. IV B is removed. This is due to the fact that the modification introduced by varying these parameters can go in the same direction or in the opposite one, depending on the observable considered. In some cases, they affect a given cosmological observable in completely different ways, e.g., some shifting the power spectrum and others affecting its amplitude (see Sec. IV). The datasets we chose are sensitive to different observables at different angular scales (lensing signal, T, E, B modes, galaxy clustering) in such a way that their combination is able to constrain these peculiar features and disentangle the degeneracies.

In Fig. 8, we show the marginalized likelihood of the model parameters $\log_{10}(\lambda-1)$ and $\log_{10}\eta$ and the impact

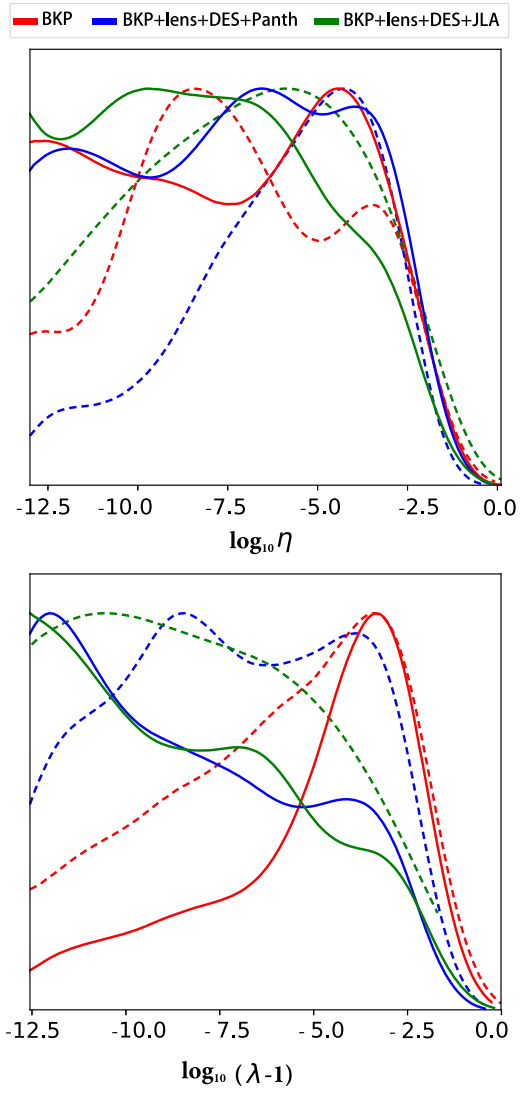

FIG. 8. The marginalized likelihood of $\log_{10}(\lambda-1)$ and $\log_{10}\eta$. Solid lines correspond to the case without massive neutrinos, dashed lines to the case with massive neutrinos.

of the different combination of datasets. We note that both parameters show a well-defined upper limit at 95% C.L. In the case of the baseline dataset, we note that λ has peaked posteriors at 68% C.L.: $\log_{10}(\lambda-1)=-2.6^{+0.1}_{-6.7}$ with massive neutrinos and $\log_{10}(\lambda-1)=-5.7\pm2.9$ without massive neutrinos. This is not the case for the posteriors of the other datasets. However, the upper limits, in these cases are stringent: $\log_{10}(\lambda-1)<-3.2$ at 95% C.L. for both datasets without massive neutrinos and $\log_{10}(\lambda-1)<-2.8$ at 95% C.L with massive neutrinos. In top panel of Fig. 8, we show the posterior of η. In the case without massive neutrinos, the datasets we considered are only able to set upper bounds, while, when massive neutrinos are included, it is also possible to obtain gaussian posteriors. In particular, for the dataset with Pth, we get $\log_{10}\eta=-6.0^{+3.4}_{-1.6}$ at 68% C.L.. In Table III, we include the bounds on the PPN parameters and G_c/G_N-1. The derived constraints for α_1 set a lower limit, which is about 1 order weaker than the PPN bound. The latter, when $\xi=1$, can be read as a constraint on η: $\log_{10}\eta<-4.1$ at 99.7% C.L. It is clear that such constraint is stronger than the ones we find using cosmological data (see Fig. 8). For α_2, we find an upper bound, which is several order of magnitude larger than the PPN constraint. Among the derived constraints on α_2, the ones from BKP seem to be the stringent ones. That is because for this dataset the bounds on λ include highest values. From Eq. (4), we can deduce that a larger value of λ decreases the estimation of α_2, as already noted in Ref. [48]. In this case also, we note that the PPN bound on $\log_{10}(\lambda-1)$ is stronger than the cosmological one. Additionally, we computed the bounds on the deviation of the effective gravitational constant from G_N, and we find that, in all cases considered, they are 2 orders of magnitude stronger than the BBN one.

We further analyzed the case in which the additional PPN bunds are considered as prior, and we find that the cosmological datasets used in this analysis do not show any improvement in the constraints.

Finally, to determine whether the Hořava gravity model is favored with respect to ΛCDM, we use the deviance information criterion (DIC) [104],

$$\mathrm{DIC} \coloneqq \chi^2_{\mathrm{eff}} + 2p_{\mathrm{D}}, \tag{16}$$

where χ^2_{eff} is the effective χ^2 corresponding to the maximum likelihood, and $p_{\mathrm{D}}=\bar{\chi}^2_{\mathrm{eff}}-\chi^2_{\mathrm{eff}}$. The bar stands for the average of the posterior distribution and can be obtained from the output chains of the MCMC analysis. The maximum likelihood is computed employing the BOBYQA algorithm, implemented in EFTCosmoMC for likelihood maximization [105]. The DIC accounts for both the goodness of fit and the bayesian complexity of the model, or, in other words, takes into account its average performance (represented by the mean likelihood). The latter can also be

considered a measure of the effective number of d.o.f. in the model.

We then compute

$$\Delta\mathrm{DIC} = \mathrm{DIC}_{\mathrm{Hor}} - \mathrm{DIC}_{\Lambda\mathrm{CDM}}. \tag{17}$$

A negative value of ΔDIC means the Hořava gravity model is supported by data over the ΛCDM one. Let us stress that both the MCMC analysis and/or the minimization algorithm for the best fit introduce statistical noise, and we must assume a scale to evaluate the ΔDIC high enough that any statistical fluke can be considered negligible when assessing the model selection criterion. Here, we consider the convention based on the Jeffreys' scale for which $\Delta\mathrm{DIC} > 10$ or >5 provide, respectively, strong and moderate evidence against the Hořava gravity model. We compute also the ΔDIC between the Hořava gravity model with and without massive neutrinos. The same Jeffreys' scale applies, where, in this case, positive values are against the presence of massive neutrinos.

We show the results in Table III. We note that the ΔDIC values between Hořava gravity and ΛCDM indicate generally a nonpreference for a particular model; *i.e.*, the data sets considered do not prefer one model over the other. Even if without a significant statistical reading, it is still of some interest the case of the analysis with the BKP data, for which the presence of massive neutrinos slows down the ΔDIC from 6.1 (moderate preference for the ΛCDM model) to −0.4. Indeed, this dataset seems to slightly favor the cosmological dynamics of Hořava gravity with massive neutrinos; however, the evidence in support of it is not sufficient to determine a proper preference between the models.

In conclusion, the model selection analysis with the considered datasets does not give a definite conclusion for the preference of one model over the other.

VI. CONCLUSION

We presented the phenomenology and observational constraints on the Hořava gravity model in Action (1) with $\xi = 1$. This model is characterized by a luminal propagation of gravitational waves in agreement with the GW170817 and GRB170817A events. We performed a phenomenological analysis of scalar angular power spectra, matter power spectrum, and primordial B-mode spectrum, focusing on the degeneracy between modification of gravity and massive neutrinos. We find that both massive neutrinos and Hořava gravity can suppress the ISW tail in the CMB TT power spectrum with respect to ΛCDM. At the same time, gravity modification enhances both the lensing and matter power spectra, while massive neutrinos mitigate these effects by suppressing the spectra amplitude. The same behavior is present in the total BB-spectrum also. In this case, another degeneracy arises among Hořava gravity parameters, massive neutrinos, and the tensor-to-scalar ratio. Indeed, large values of both r and Hořava gravity parameters can enhance the primordial total BB spectra, while a nonzero massive neutrinos component can suppress this feature. The effects of a modified background evolution impact the high-ℓTT power spectrum in different ways: by shifting the peaks to high multipoles and in the height of the CMB peaks, which are suppressed due to an early ISW effect. Massive neutrinos instead shift the spectrum to lower multipoles. Thus, a fine-tuning among the mass of neutrinos and the values of Hořava parameters can, in principle, compensate. The impact on the tensor BB-power spectrum are instead peculiar in the two cases; modification of gravity suppresses peaks and troughs, while massive neutrinos further suppress the first peak, but they enhance the spectrum for larger multipoles. We used CMB, SNIa, galaxy clustering, and weak gravitational lensing measurements in different combinations, and we find that they were able to break these degeneracy due to the power in constraining different features of the model.

We provided observational constraints on model and cosmological parameters in the Hořava gravity model using these data. We found that the cosmological parameters are compatible with those of ΛCDM in both scenarios (with or without massive neutrinos). As such, the tensions in H_0 and σ_8^0 between low-redshift and CMB data are not alleviated in Hořava gravity. The models parameters are severely constrained to be their GR limits. However, their constraints are weaker than the ones obtained from the PPN bounds. We also computed the bounds on the deviation of the effective gravitational constant, G_c from the Newtonian one G_N, and we found it to be 2 order of magnitude stringent than the PPN one regardless of the dataset considered.

The model selection analysis using the deviance information criterion (DIC) suggests that CMB data from Planck 2018, BICEP2, and Keck Array experiments prefer in the case of Hořava gravity $\Sigma m_\nu \neq 0$ ($\Delta\mathrm{DIC} = -3$); the opposite holds for the extended analysis, in particular, for the combination of data including the JLA dataset. The CMB data are the only ones which slightly prefer the Hořava gravity model with massive neutrinos over the ΛCDM ($\Delta\mathrm{DIC} = -0.4$), even though without a significant statistical evidence, in all other cases (with or without massive neutrinos), there is either a mild preference for ΛCDM ($\Delta\mathrm{DIC} = 6.1$ for BKP without massive neutrinos, $\Delta\mathrm{DIC} = 4.1$ for BKP + lens + DES + JLA with massive neutrinos) or a null preference.

In conclusion, the Hořava gravity model can be still considered a viable candidate to explain the late time acceleration of the Universe, and it deserves further investigations particularly once new data will be available from next generation surveys, such as Euclid [106], DESI [107], LSST [108], SKA [109,110], COrE [111], and CMB-S4 [112,113]. These surveys will allow one to measure

cosmological and model parameters with unprecedented accuracy and can help to definitely discriminate among the different cosmological models.

ACKNOWLEDGMENTS

We thank Bin Hu and Daniele Vernieri for useful discussions and comments on the manuscript. N. F. is supported by Fundação para a Ciência e a Tecnologia (FCT) through the research Grants No. UID/FIS/04434/2019, No. UIDB/04434/2020 and No. UIDP/04434/2020 and by FCT project "DarkRipple—Spacetime ripples in the dark gravitational Universe" with Ref. No. PTDC/FIS-OUT/29048/2017. M. B. acknowledges Istituto Nazionale di Fisica Nucleare (INFN), sezione di Napoli, iniziativa specifica QGSKY. This work was developed thanks to the High Performance Computing Center at the Universidade Federal do Rio Grande do Norte (NPAD/UFRN) and the National Observatory (ON) computational support. This paper is based upon work from COST Action (CANTATA/CA15117), supported by COST (European Cooperation in Science and Technology).

[1] S. Weinberg, Rev. Mod. Phys. **61**, 1 (1989).
[2] J. Martin, C.R. Phys. **13**, 566 (2012).
[3] A. Joyce, B. Jain, J. Khoury, and M. Trodden, Phys. Rep. **568**, 1 (2015).
[4] S. M. Carroll, Living Rev. Relativity **4**, 1 (2001).
[5] S. Weinberg, in *4th International Symposium on Sources and Detection of Dark Matter in the Universe (DM 2000)* (2000), https://www.springer.com/gp/book/9783540412168.
[6] A. Padilla, arXiv:1502.05296.
[7] A. G. Riess, S. Casertano, W. Yuan, L. M. Macri, and D. Scolnic, Astrophys. J. **876**, 85 (2019).
[8] K. C. Wong *et al.*, Mon. Not. R. Astron. Soc. **498**, 1420 (2020).
[9] T. Delubac *et al.* (BOSS Collaboration), Astron. Astrophys. **574**, A59 (2015).
[10] K. S. Dawson *et al.* (BOSS Collaboration), Astron. J. **145**, 10 (2013).
[11] K. N. Abazajian *et al.* (SDSS Collaboration), Astrophys. J. Suppl. Ser. **182**, 543 (2009).
[12] W. L. Freedman *et al.*, Astrophys. J. **882**, 34 (2019).
[13] W. Yuan, A. G. Riess, L. M. Macri, S. Casertano, and D. Scolnic, Astrophys. J. **886**, 61 (2019).
[14] J. T. A. de Jong *et al.*, Astron. Astrophys. **582**, A62 (2015).
[15] N. Aghanim *et al.* (Planck Collaboration), Astron. Astrophys. **641**, A6 (2020).
[16] G. W. Horndeski, Int. J. Theor. Phys. **10**, 363 (1974).
[17] Y. Fujii and K. Maeda, *The Scalar-Tensor Theory of Gravitation*, Cambridge Monographs on Mathematical Physics (Cambridge University Press, Cambridge, England, 2007), ISBN 9780521037525, 9780521811590, 9780511029882.
[18] C. Deffayet, S. Deser, and G. Esposito-Farese, Phys. Rev. D **80**, 064015 (2009).
[19] T. Clifton, P. G. Ferreira, A. Padilla, and C. Skordis, Phys. Rep. **513**, 1 (2012).
[20] S. Tsujikawa, Lect. Notes Phys. **800**, 99 (2010).
[21] J. Gleyzes, D. Langlois, F. Piazza, and F. Vernizzi, Phys. Rev. Lett. **114**, 211101 (2015).
[22] K. Koyama, Rep. Prog. Phys. **79**, 046902 (2016).
[23] D. Langlois and K. Noui, J. Cosmol. Astropart. Phys. 02 (2016) 034.
[24] P. G. Ferreira, Annu. Rev. Astron. Astrophys. **57**, 335 (2019).
[25] N. Frusciante and L. Perenon, Phys. Rep. **857**, 1 (2020).
[26] P. Horava, J. High Energy Phys. 03 (2009) 020.
[27] P. Horava, Phys. Rev. D **79**, 084008 (2009).
[28] M. Visser, Phys. Rev. D **80**, 025011 (2009).
[29] M. Visser, arXiv:0912.4757.
[30] T. P. Sotiriou, J. Phys. Conf. Ser. **283**, 012034 (2011).
[31] T. P. Sotiriou, M. Visser, and S. Weinfurtner, J. High Energy Phys. 10 (2009) 033.
[32] C. Charmousis, G. Niz, A. Padilla, and P. M. Saffin, J. High Energy Phys. 08 (2009) 070.
[33] D. Blas, O. Pujolas, and S. Sibiryakov, J. High Energy Phys. 10 (2009) 029.
[34] A. Wang and R. Maartens, Phys. Rev. D **81**, 024009 (2010).
[35] N. Afshordi, Phys. Rev. D **80**, 081502 (2009).
[36] K. Koyama and F. Arroja, J. High Energy Phys. 03 (2010) 061.
[37] D. Vernieri and T. P. Sotiriou, Phys. Rev. D **85**, 064003 (2012).
[38] D. Vernieri and T. P. Sotiriou, J. Phys. Conf. Ser. **453**, 012022 (2013).
[39] D. Vernieri, Phys. Rev. D **91**, 124029 (2015).
[40] D. Blas, O. Pujolas, and S. Sibiryakov, Phys. Rev. Lett. **104**, 181302 (2010).
[41] S. M. Carroll and E. A. Lim, Phys. Rev. D **70**, 123525 (2004).
[42] J. A. Zuntz, P. G. Ferreira, and T. G. Zlosnik, Phys. Rev. Lett. **101**, 261102 (2008).
[43] T. Kobayashi, Y. Urakawa, and M. Yamaguchi, J. Cosmol. Astropart. Phys. 04 (2010) 025.
[44] C. Armendariz-Picon, N. F. Sierra, and J. Garriga, J. Cosmol. Astropart. Phys. 07 (2010) 010.
[45] D. Blas, M. M. Ivanov, and S. Sibiryakov, J. Cosmol. Astropart. Phys. 10 (2012) 057.
[46] B. Audren, D. Blas, J. Lesgourgues, and S. Sibiryakov, J. Cosmol. Astropart. Phys. 08 (2013) 039.
[47] B. Audren, D. Blas, M. M. Ivanov, J. Lesgourgues, and S. Sibiryakov, J. Cosmol. Astropart. Phys. 03 (2015) 016.

[48] N. Frusciante, M. Raveri, D. Vernieri, B. Hu, and A. Silvestri, Phys. Dark Universe **13**, 7 (2016).
[49] D. Munshi, B. Hu, T. Matsubara, P. Coles, and A. Heavens, J. Cosmol. Astropart. Phys. 04 (2016) 056.
[50] Y. Gong, S. Hou, E. Papantonopoulos, and D. Tzortzis, Phys. Rev. D **98**, 104017 (2018).
[51] X.-L. Chen, R. J. Scherrer, and G. Steigman, Phys. Rev. D **63**, 123504 (2001).
[52] J. W. Elliott, G. D. Moore, and H. Stoica, J. High Energy Phys. 08 (2005) 066.
[53] C. M. Will, Living Rev. Relativity **17**, 4 (2014).
[54] J. F. Bell, F. Camilo, and T. Damour, Astrophys. J. **464**, 857 (1996).
[55] D. Blas, O. Pujolas, and S. Sibiryakov, J. High Energy Phys. 04 (2011) 018.
[56] D. Blas and H. Sanctuary, Phys. Rev. D **84**, 064004 (2011).
[57] M. Bonetti and E. Barausse, Phys. Rev. D **91**, 084053 (2015); **93**, 029901(E) (2016).
[58] K. Yagi, D. Blas, E. Barausse, and N. Yunes, Phys. Rev. D **89**, 084067 (2014); **90**, 069902(E) (2014); **90**, 069901(E) (2014).
[59] B. Abbott *et al.* (Virgo and LIGO Scientific Collaborations), Phys. Rev. Lett. **119**, 161101 (2017).
[60] B. P. Abbott *et al.* (Virgo, Fermi-GBM, INTEGRAL, LIGO Scientific Collaborations), Astrophys. J. **848**, L13 (2017).
[61] A. E. Gumrukcuoglu, M. Saravani, and T. P. Sotiriou, Phys. Rev. D **97**, 024032 (2018).
[62] H. Motohashi, A. A. Starobinsky, and J. Yokoyama, Phys. Rev. Lett. **110**, 121302 (2013).
[63] J.-H. He, Phys. Rev. D **88**, 103523 (2013).
[64] M. Baldi, F. Villaescusa-Navarro, M. Viel, E. Puchwein, V. Springel, and L. Moscardini, Mon. Not. R. Astron. Soc. **440**, 75 (2014).
[65] B. Hu, M. Raveri, A. Silvestri, and N. Frusciante, Phys. Rev. D **91**, 063524 (2015).
[66] H. Motohashi, A. A. Starobinsky, and J. Yokoyama, Prog. Theor. Phys. **124**, 541 (2010).
[67] N. Bellomo, E. Bellini, B. Hu, R. Jimenez, C. Pena-Garay, and L. Verde, J. Cosmol. Astropart. Phys. 02 (2017) 043.
[68] D. Alonso, E. Bellini, P. G. Ferreira, and M. Zumalacárregui, Phys. Rev. D **95**, 063502 (2017).
[69] N. Frusciante, S. Peirone, L. Atayde, and A. De Felice, Phys. Rev. D **101**, 064001 (2020).
[70] B. S. Wright, K. Koyama, H. A. Winther, and G.-B. Zhao, J. Cosmol. Astropart. Phys. 06 (2019) 040.
[71] T. Jacobson, Proc. Sci., QG-PH2007 (**2007**) 020 [arXiv: 0801.1547].
[72] Y. I. Izotov, T. X. Thuan, and N. G. Guseva, Mon. Not. R. Astron. Soc. **445**, 778 (2014).
[73] E. Aver, K. A. Olive, and E. D. Skillman, J. Cosmol. Astropart. Phys. 07 (2015) 011.
[74] C. Patrignani *et al.* (Particle Data Group), Chin. Phys. C **40**, 100001 (2016).
[75] G. Gubitosi, F. Piazza, and F. Vernizzi, J. Cosmol. Astropart. Phys. 02 (2013) 032.
[76] J. K. Bloomfield, E. E. Flanagan, M. Park, and S. Watson, J. Cosmol. Astropart. Phys. 08 (2013) 010.
[77] J. Gleyzes, D. Langlois, F. Piazza, and F. Vernizzi, J. Cosmol. Astropart. Phys. 08 (2013) 025.
[78] F. Piazza, H. Steigerwald, and C. Marinoni, J. Cosmol. Astropart. Phys. 05 (2014) 043.
[79] S. Tsujikawa, Lect. Notes Phys. **892**, 97 (2015).
[80] B. Hu, M. Raveri, N. Frusciante, and A. Silvestri, Phys. Rev. D **89**, 103530 (2014).
[81] M. Raveri, B. Hu, N. Frusciante, and A. Silvestri, Phys. Rev. D **90**, 043513 (2014).
[82] B. Hu, M. Raveri, N. Frusciante, and A. Silvestri, arXiv:1405.3590.
[83] N. Frusciante, G. Papadomanolakis, and A. Silvestri, J. Cosmol. Astropart. Phys. 07 (2016) 018.
[84] J. Lesgourgues and S. Pastor, Phys. Rep. **429**, 307 (2006).
[85] Y. Y. Y. Wong, Annu. Rev. Nucl. Part. Sci. **61**, 69 (2011).
[86] M. Lattanzi (Planck Collaboration), J. Phys. Conf. Ser. **718**, 032008 (2016).
[87] M. Aker *et al.* (KATRIN Collaboration), Phys. Rev. Lett. **123**, 221802 (2019).
[88] A. Lewis and A. Challinor, Phys. Rev. D **66**, 023531 (2002).
[89] R.-G. Cai, B. Hu, and H.-B. Zhang, Phys. Rev. D **80**, 041501 (2009).
[90] Y. Akrami *et al.* (Planck Collaboration), Astron. Astrophys. **641**, A10 (2020).
[91] N. Aghanim *et al.* (Planck Collaboration), Astron. Astrophys. **641**, A5 (2020).
[92] P. A. R. Ade *et al.* (BICEP2, Keck Array Collaborations), Phys. Rev. Lett. **121**, 221301 (2018).
[93] V. Pettorino and L. Amendola, Phys. Lett. B **742**, 353 (2015).
[94] N. Aghanim *et al.* (Planck Collaboration), Astron. Astrophys. **641**, A8 (2020).
[95] M. Betoule *et al.* (SDSS Collaboration), Astron. Astrophys. **568**, A22 (2014).
[96] L. Taddei, M. Martinelli, and L. Amendola, J. Cosmol. Astropart. Phys. 12 (2016) 032.
[97] M. Benetti, W. Miranda, H. A. Borges, C. Pigozzo, S. Carneiro, and J. S. Alcaniz, J. Cosmol. Astropart. Phys. 12 (2019) 023.
[98] D. M. Scolnic *et al.*, Astrophys. J. **859**, 101 (2018).
[99] T. M. C. Abbott *et al.* (DES Collaboration), Phys. Rev. D **98**, 043526 (2018).
[100] A. De Felice, N. Frusciante, and G. Papadomanolakis, J. Cosmol. Astropart. Phys. 03 (2017) 027.
[101] N. Frusciante, G. Papadomanolakis, S. Peirone, and A. Silvestri, J. Cosmol. Astropart. Phys. 02 (2019) 029.
[102] T. M. C. Abbott *et al.* (DES Collaboration), Mon. Not. R. Astron. Soc. **480**, 3879 (2018).
[103] M. Asgari *et al.*, Astron. Astrophys. **634**, A127 (2020).
[104] D. J. Spiegelhalter, N. G. Best, B. P. Carlin, and A. van der Linde, J. R. Stat. Soc. **76**, 485 (2014).
[105] M. Powell, The BOBYQA algorithm for bound constrained optimization without derivatives, Vol. Report DAMTP 2009/NA06, 2009.
[106] L. Amendola *et al.*, Living Rev. Relativity **21**, 2 (2018).
[107] M. E. Levi *et al.* (DESI Collaboration), arXiv:1907.10688.
[108] S. W. Jha *et al.*, arXiv:1907.08945.

[109] R. Maartens, F. B. Abdalla, M. Jarvis, and M. G. Santos (SKA Cosmology SWG), Proc. Sci., AASKA14 (**2015**) 016 [arXiv:1501.04076].
[110] D. J. Bacon *et al.* (SKA Collaboration), Pub. Astron. Soc. Aust. **37**, e007 (2020).
[111] E. Di Valentino *et al.* (CORE Collaboration), J. Cosmol. Astropart. Phys. 04 (2018) 017.
[112] K. Abazajian *et al.*, Bull. Am. Astron. Soc. **51**, 209 (2019).
[113] K. Abazajian *et al.*, arXiv:1907.04473.